# On the Electronic Structure of $NLi_2$ and $PLi_2$, Ground and Low-Lying Excited States

**Demeter Tzeli, Aristotle Papakondylis, and Aristides Mavridis***

*Laboratory of Physical Chemistry, Department of Chemistry, National and Kapodistrian University of Athens, P.O. Box 64004, 15710 Zografou, Athens, Greece*

*Received: September 12, 1997; In Final Form: December 3, 1997*

The ground states of the isovalent molecules $NLi_2$ ($\tilde{X}^2\Pi_u$) and $PLi_2$ ($\tilde{X}^2B_1$), along with some low-lying excited states ($^2B_2$,$^4\Sigma_g^-$, $^2\Sigma_g^-$, $^4\Sigma_u^-$, $^2\Sigma_u^-$, and $^2A_1$), have been examined using ab initio CISD, CASSCF, and MRCI methods in conjunction with relatively large correlation consistent basis sets. We report total energies, geometries, binding energies, Mulliken charges, energy gaps, and for certain states, potential energy curves. All states examined are bound with respect to the ground-state atoms N or P($^4$S) + 2Li($^2$S), while the mean binding energies N−Li and P−Li of $NLi_2$ and $PLi_2$ are 42.5 and 40.2 kcal/mol, respectively.

## 1. Introduction

In the present report we examine via ab initio methods the electronic structure of the ground state and of some low-lying excited states of the isovalent molecules dilithium nitride ($NLi_2$) and dilithium phosphide ($PLi_2$). To the best of our knowledge there are no experimental or theoretical results in the literature for $NLi_2$. The $PLi_2$ system has been observed in the gas phase by Knudsen-effusion mass spectrometry,[1] along with other phosphorus-lithiated species. We are also aware of some, as yet unpublished, ab initio results by Kudo[2] on the ground states of PLi and $PLi_2$ molecules (vide infra). On the other hand, experimental results on lithiated N- and P-species in the solid state have existed for quite a few years.[3] The interest in these systems is due to their ionic nature and the role they could potentially play as solid-state ionic conductors.

Using SCF, CISD(+corrections), CASSCF (complete active space SCF), CASSCF+1+2 (CASSCF + single + double replacements = MRCI), and MRCI+corrections methods in conjuction with rather large correlation consistent basis sets, we have examined the ground states $\tilde{X}^2\Pi_u(NLi_2)$ and $\tilde{X}^2B_1$-($PLi_2$), as well as the low-lying excited states $^2B_2$, $^2\Sigma_g^-$, $^2\Sigma_u^-$, $^2A_1$, $^4\Sigma_g^-$, and $^4\Sigma_u^-$ for both title molecules. In an effort to better understand the nature of the chemical bond in these unusual species, we have also constructed potential energy curves (PECs) for certain states; in particular for the ground $^2\Pi_u$ state of $NLi_2$ we constructed PECs referring to both dissociation channels, $NLi_2 \rightarrow NLi + Li$ and $NLi_2 \rightarrow N + 2Li$.

The present report is a continuation of our work on lithiated species;[4] we believe that the simplicity of the Li atom (one active electron), in parallel with its low-lying first excited state ($\Delta E(^2P \leftarrow ^2S) = 1.85$ eV), presents an ideal case for the study of the chemical bond.

## 2. Basis Sets and Methods

For all atoms, the correlation consistent polarized basis sets of Dunning were used, cc-pV*n*Z, where *n* is a cardinal number characterizing the basis set quality.[5,6] One of the nicest properties of the cc-bases is their potential of improving in a well-defined and systematic way the quality of calculation and their convergence toward the "complete basis set" limits of various molecular properties within the methodology employed.[7]

For the N and P atoms the quadruple $n = 4$ (QZ) quality basis was employed but with the functions of g-symmetry removed (cc-pVQZ-g). For the N atom only and in conjuction with the CISD method, the augmented cc-pVQZ-g (cc-pVQZ + one diffuse function for each symmetry present = aug-cc-pVQZ-g) was used. For the Li atom the $n = 3$(TZ) basis was selected. For instance, the $PLi_2$ basis set reads as follows: (16s11p3d2f/(11s5p2d1f)$_2$) → [6s5p3d2f/(4s3p2d1f)$_2$], comprised of 110 contracted spherical Gaussians (i.e., five d and seven f functions). The reason for selecting these particular bases, e.g., $n = 4$ for the N and P atoms and $n = 3$ for the Li atom, will be discussed further in the next section.

As was already mentioned, the theoretical methodologies employed are SCF, CISD(SCF+1+2), CASSCF, and CASSCF+1+2 (MRCI). In the CASSCF calculations, the Li 2s-, N 2s2p-, and P 3s3p-like orbitals were included in the active space. The Li 1s-, N 1s-, and P 1s2s2p-like orbitals were optimized but always constrained to be doubly occupied. Given those restrictions, our CASSCF space for the triatomic species contains seven active orbitals and seven (valence) electrons. Depending on the symmetry of the state, the size of the CAS space ranges from 112 ($^4\Sigma_g^-$) to 404 ($^2A_1$) CSFs, with 988 665 and 1 501 544 CSFs, respectively, in the MRCI space. No corrections for basis set superposition errors were applied, assuming that the size of the basis sets was large enough. It should also be mentioned that the size extensivity error in all MRCI PECs studied was less than 0.1 mhartree.

Our computations were performed with the COLUMBUS[8] suite, with some CISD results checked by the MELD[9] code. Also, the MOLPRO[10,11] code was used for certain calculations on the diatomic molecule NLi.

## 3. Results and Discussion

**a. The Diatomics NLi and PLi.** Recently we have reported on the ground and low-lying states of NLi[4b] and PLi[4a] molecules. With the purpose of selecting basis sets of adequate size for the triatomic species $NLi_2$ and $PLi_2$, while at the same time keeping our calculations manageable, we have reexamined the dissociation energies ($D_e$) and bond lengths ($r_e$) of NLi and PLi ground states as a function of basis set size. Our results at the MRCI level, along with literature results, are reported in Table 1. Considering the $D_e$ and $r_e$ as the most sensitive parameters

S1089-5639(97)02998-8 CCC: $15.00 
Published on Web 02/28/1998

**TABLE 1: MRCI Results on the Ground $X^3\Sigma^-$ State of NLi and PLi as a Function of Basis Set Size: Energies (hartrees), Bond Distances $r_e$ (angstroms), Dissociation Energies $D_e$ (kcal/mol), and Harmonic Frequencies $\omega_e$ ($cm^{-1}$)**

| basis set | $-E$ | $r_e$ | $D_e$ | $\omega_e$ |
|---|---|---|---|---|
| | NLi | | | |
| aug-cc-pVTZ/DZ[a] | 61.98909 | 1.921 | 29.5 | 619.9 |
| cc-pVQZ-g/cc-pVTZ | 62.00663 | 1.885 | 33.3 | 655.2 |
| cc-pVQZ/cc-pVTZ[b] | 62.00774 | 1.879 | 33.5 | 663.2 |
| cc-pVQZ-g/cc-pVQZ-g | 62.00786 | 1.881 | 34.1 | 660.1 |
| aug-cc-pVQZ-g/cc-pVTZ | 62.00884 | 1.889 | 34.5 | 649.9 |
| cc-pV5Z/cc-pVQZ[b] | 62.01347 | 1.877 | 35.4 | 665.3 |
| aug-cc-pV5Z/cc-pVQZ[b] | 62.01451 | 1.879 | 35.8 | 662.2 |
| DZ+P-Slater functions[c] | 61.7781 | 1.85 | 19.6 | 657 |
| 6-311+G(2df)//6-31+G*[d] | *d* | 1.874[e] | 34.4[d] | 681[e] |
| | PLi | | | |
| cc-pVQZ-g/cc-pVTZ | 348.31423 | 2.357 | 36.3 | 476.8 |
| cc-pVQZ-g/cc-pVQZ-g[f] | 348.31497 | 2.351 | 36.8 | 479.1 |
| aug-cc-pVQZ-g/cc-pVQZ-g | 348.31554 | 2.353 | 37.1 | 478.7 |
| 6-311+G(2df)[g] | 348.30484 | 2.342 | 38.4 | 495[h] |
| [5s4p2d/4s3p2d][i] | 348.29936 | 2.372 | | |

[a] Reference 4b. [b] Internally contracted MRCI, MOLPRO code. [c] Reference 12, CISD with respect to a two-configuration reference. [d] Reference 13a, QCISD(T), 6-311+G(2df)//MP2(full/6-31+G*), no absolute energy value is given. [e] Reference 13a, MP2(full)/6-311+G*. [f] Reference 4a. [g] Reference 13b, QCISD(T). [h] Reference 13b, MP2(full)/6-31+G*. [i] Reference 2, MRCI+Full-CI Davidson correction, contracted ANO-basis set (17s12p5d4f/14s9p4d3f) → [5s4p2d/4s3p2d].

with respect to the basis set size, Table 1 reveals that for NLi our best results, $D_e = 35.8$ kcal/mol and $r_e = 1.879$ Å, are in fair agreement with the cc-pVQZ-g/cc-pVTZ numbers, that is, $D_e = 33.3$ kcal/mol and $r_e = 1.884$ Å. Incidentally, the $D_e$ value of NLi in the aug-cc-pV5Z/cc-pVQZ basis is the most accurate reported so far in the literature.

Similarly, results on the PLi molecule are presented in Table 1, from where it is obvious that the cc-pVQZ-g/cc-pVTZ numbers are in good agreement with the more flexible basis sets.

The above results rationalize our selection of the QZ-g/TZ basis in the treatment of both triatomic species, $NLi_2$ and $PLi_2$.

Table 2 summarizes all relevant arithmetic results on NLi and PLi for the ground $X^3\Sigma^-$ and the first excited $A^3\Pi$ states in the QZ-g/TZ basis, using different methodologies. Analysis of similar results with that of Table 2 (with a smaller and slightly larger basis set for NLi and PLi, respectively) and binding mechanisms can be found elsewhere.[4a,b] The only purpose of presenting Table 2 is its relevance in discussing the triatomics $NLi_2$ and $PLi_2$. A few comments though are in order. Both molecules in both states are ionic with almost half an electron transferred from Li to N or P in the $X^3\Sigma^-$ state(s); in the $X^3\Sigma^-$ state(s) there is a single bond of $\sigma$-character, while in the $A^3\Pi$ state(s) the atoms are held together by a $\pi$-bond, a half $\sigma$-bond, and a half $\pi$-bond (by a half-bond we mean that only one electron is involved in the bonding process). It should also be mentioned that the $A^3\Pi$ state correlates to $N(^4S) + Li(^2P)$ or $P(^2D) + Li(^2S)$ fragments. This double-bond character of the $A^3\Pi$ state(s) is reflected in the impressive bond length shortening along with a significant increase in the $D_e$ values (with respect to the asymptotic products) as compared to the $X^3\Sigma^-$ state, Table 2.

**b. The Triatomics $NLi_2$ and $PLi_2$.** Tables 3 and 4 present numerical results on $NLi_2$ and $PLi_2$, respectively; we report total energies, equilibrium geometries, dissociation energies with respect to the ground-state fragments N or P ($^4S$) + 2Li($^2S$), Mulliken charges, and energy gaps of the ground and some low-lying excited states and in different methodologies. In what

**TABLE 2: Absolute Energies *E* (hartrees), Bond Lengths $r_e$ (angstroms), Dissociation Energies $D_e$ (kcal/mol), Mulliken Charges *q* (N or P), and Energy Differences $T_e$ (kcal/mol) of NLi and PLi in the $X^3\Sigma^-$ and $A^3\Pi$ States**

| method | $-E$ | $r_e$ | $D_e$[c] | *q* | $T_e$ |
|---|---|---|---|---|---|
| | | NLi($X^3\Sigma^-$) | | | |
| SCF | 61.833 53 | 1.844 | 0.4 | −0.54 | |
| CISD | 62.001 73 | 1.873 | 30.9 | −0.55 | |
| CISD+Q[a] | 62.013 | 1.886 | 35 | | |
| CASSCF | 61.868 89 | 1.900 | 15.5 | −0.51 | |
| MRCI | 62.006 63 | 1.885 | 33.3 | −0.50 | |
| MRCI+Q[b] | 62.014 | 1.890 | 35 | | |
| | | NLi($A^3\Pi$) | | | |
| CASSCF | 61.862 95 | 1.734 | 54.2 | −0.40 | 3.7 |
| MRCI | 61.998 25 | 1.737 | 70.5 | −0.41 | 5.3 |
| MRCI+Q[b] | 62.005 | 1.740 | 72 | | 5.4 |
| | | PLi($X^3\Sigma^-$) | | | |
| SCF | 348.173 80 | 2.342 | 14.3 | −0.45 | |
| CISD | 348.308 77 | 2.339 | 34.0 | −0.43 | |
| CISD+Q[a] | 348.320 | 2.344 | 37 | | |
| CASSCF | 348.198 88 | 2.400 | 21.3 | −0.39 | |
| MRCI | 348.314 23 | 2.357 | 36.3 | −0.41 | |
| MRCI+Q[b] | 348.323 | 2.356 | 38 | | |
| | | PLi($A^3\Pi$) | | | |
| CASSCF | 348.180 67 | 2.219 | 40.0 | −0.40 | 11.4 |
| MRCI | 348.292 46 | 2.227 | 56.9 | −0.34 | 13.7 |
| MRCI+Q[b] | 348.301 | 2.231 | 59 | | 14.1 |

[a] Single-reference Davidson correction for unlinked quadruples. [b] Multireference Davidson correction, ref 14. [c] $X^3\Sigma^-$, $D_e$ with respect to the ground-state products. $A^3\Pi$, $D_e$ with respect to asymptotic products, i.e., NLi($A^3\Pi$) → $N(^4S)$ + $Li(^2P)$ and PLi($A^3\Pi$) → $P(^2D)$ + $Li(^2S)$.

follows we analyze our findings with an emphasis on the binding mechanisms.

**$NLi_2$, Ground $\tilde{X}^2\Pi_u$ ($1\sigma_g^2 2\sigma_g^2 1\sigma_u^2 3\sigma_g^2 2\sigma_u^2 1\pi_u^3$) State.** We imagine that the molecule is formed either by a ground-state $Li(^2S)$ atom approaching the first excited $A^3\Pi$ state of NLi or by a Li atom in its excited $^2P$ state approaching the ground $X^3\Sigma^-$ of NLi. A clear visualization of these two routes is obtained by using valence bond−Lewis icons. Of course, at equilibrium,

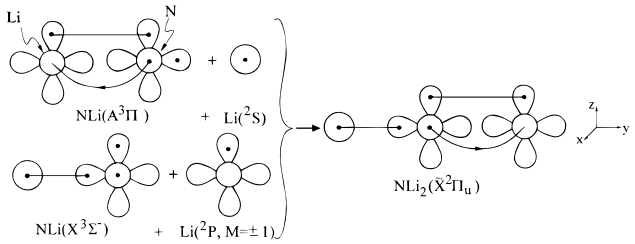


both the above molecular picture and its mirror image are present, so the two Li atoms are strictly equivalent. At equilibrium the CAS atomic populations are

$$\text{N:}\quad 2s^{1.73}2p_x^{0.88}2p_y^{1.37}2p_z^{1.44}$$

$$\text{Li:}\quad 2s^{0.22}2p_x^{0.04}2p_y^{0.11}2p_z^{0.31}$$

in reasonal agreement with the above picture. Each Li atom is losing 0.66 $e^-$ via the $\sigma$-frame gaining at the same time 0.35 $e^-$ via the $\pi$-frame; overall, ~0.4 $e^-$ are transferred to the N atom. Bending the molecule results in the two nondegenerate components (Renner−Teller splitting) $^2B_1(3a_1^2 4a_1^2 1b_1^1 2b_2^2)$ and $^2A_1(3a_1^2 4a_1^1 1b_1^2 2b_2^2)$, degenerate in the linear $|\Lambda| = 1$ geometry, Figure 1. We observe that $NLi_2$ is a very floppy molecule, requiring just 0.6 mhartree to bend it up to 140° on the $^2B_1$ surface.

**TABLE 3: Absolute Energies $E$ (hartrees), Bond Lengths $r_e$ (angstroms), Angles $\theta$ (degrees ∠LiNLi), Binding Energies $D_e$ (kcal/mol), Mulliken Charges $q_N$, and Energy Differences $T_e$ (kcal/mol) of the Ground $^2\Pi_u$ State and Some Low-Lying Excited States of $NLi_2$**

| method | $-E$ | $r_e$ | $\theta$ | $D_e$[a] | $q$ | $T_e$[b] |
|---|---|---|---|---|---|---|
| | | | $\tilde{X}^2\Pi_u$ | | | |
| SCF | 69.290 85 | 1.746 | 180.0 | 15.9 | −0.57 | |
| CISD | 69.505 84 | 1.767 | 180.0 | 75.5 | −0.58 | |
| CISD+Q[c] | 69.523 | 1.777 | 180.0 | 83 | | |
| CASSCF | 69.375 71 | 1.790 | 180.0 | 62.0 | −0.43 | |
| MRCI | 69.521 59 | 1.782 | 180.0 | 84.9 | −0.45 | |
| MRCI+Q[d] | 69.530 | 1.786 | 180.0 | 88 | | |
| | | | $^2B_2$ | | | |
| SCF | 69.268 38 | 1.671 | 140.2 | 1.8 | −0.50 | 14.1 |
| CISD | 69.487 24 | 1.702 | 125.8 | 63.8 | −0.47 | 11.7 |
| CISD+Q[c] | 69.506 | 1.715 | 123.2 | 73 | | 10.8 |
| CASSCF | 69.361 01 | 1.722 | 118.4 | 52.8 | −0.41 | 9.2 |
| MRCI | 69.506 15 | 1.738 | 111.4 | 75.3 | −0.45 | 9.7 |
| MRCI+Q[d] | 69.515 | 1.750 | 106.4 | 78 | | 9.9 |
| | | | $^2\Sigma_u^+$ [e] | | | |
| SCF | 69.267 93 | 1.660 | 180.0 | | −0.53 | 14.4 |
| CISD | 69.484 62 | 1.678 | 180.0 | | −0.53 | 13.3 |
| CISD+Q[c] | 69.502 | 1.686 | 180.0 | | | 13.1 |
| CASSCF | 69.358 55 | 1.684 | 180.0 | | −0.32 | 10.8 |
| MRCI | 69.502 57 | 1.689 | 180.0 | | −0.35 | 11.9 |
| MRCI+Q[d] | 69.510 | 1.693 | 180.0 | | | 12.6 |
| | | | $^4\Sigma_g^-$ | | | |
| SCF | 69.307 62 | 1.925 | 180.0 | 26.4 | −0.37 | −10.5 |
| CISD | 69.478 53 | 1.912 | 180.0 | 58.3 | −0.33 | 17.1 |
| CISD+Q[c] | 69.489 | 1.921 | 180.0 | 62 | | 21.5 |
| CASSCF | 69.342 27 | 1.930 | 180.0 | 41.0 | −0.34 | 21.0 |
| MRCI | 69.483 93 | 1.921 | 180.0 | 61.3 | −0.32 | 23.6 |
| MRCI+Q[d] | 69.492 | 1.925 | 180.0 | 64 | | 24.2 |
| | | | $^2\Sigma_g^-$ | | | |
| SCF | 69.304 03 | 1.895 | 180.0 | 24.1 | −0.40 | −8.3 |
| CISD | 69.474 38 | 1.924 | 180.0 | 55.7 | −0.36 | 19.7 |
| CISD+Q[c] | 69.485 | 1.933 | 180.0 | 59 | | 24.1 |
| CASSCF | 69.339 08 | 1.943 | 180.0 | 39.0 | −0.35 | 23.0 |
| MRCI | 69.478 56 | 1.928 | 180.0 | 57.9 | −0.35 | 27.0 |
| MRCI+Q[d] | 69.486 | 1.931 | 180.0 | 60 | | 27.9 |
| | | | $^4\Sigma_u^-$ | | | |
| SCF | 69.296 84 | 1.908 | 180.0 | 19.6 | −0.28 | −3.8 |
| CISD | 69.466 03 | 1.930 | 180.0 | 50.5 | −0.28 | 25.0 |
| CISD+Q[c] | 69.476 | 1.938 | 180.0 | 54 | | 29.6 |
| CASSCF | 69.332 05 | 1.946 | 180.0 | 34.6 | −0.36 | 27.4 |
| MRCI | 69.471 50 | 1.940 | 180.0 | 53.5 | −0.36 | 31.4 |
| MRCI+Q[d] | 69.479 | 1.944 | 180.0 | 56 | | 32.4 |
| | | | $^2\Sigma_u^-$ | | | |
| SCF | 69.295 78 | 1.908 | 180.0 | 18.9 | −0.28 | −3.1 |
| CISD | 69.464 67 | 1.929 | 180.0 | 49.6 | −0.26 | 25.8 |
| CISD+Q[c] | 69.474 | 1.936 | 180.0 | 53 | | 31 |
| CASSCF | 69.330 68 | 1.943 | 180.0 | 33.7 | −0.37 | 28.3 |
| MRCI | 69.470 00 | 1.936 | 180.0 | 52.6 | −0.36 | 32.4 |
| MRCI+Q[d] | 69.477 | 1.939 | 180.0 | 55 | | 33 |
| | | | $^2A_1$ | | | |
| SCF | 69.229 21 | 1.937 | 89.1 | −22.8 | −0.24 | 38.7 |
| CISD | 69.418 40 | 1.954 | 88.4 | 20.6 | −0.24 | 54.9 |
| CISD+Q[c] | 69.434 | 1.962 | 88.4 | 28 | | 55.9 |
| CASSCF | 69.304 24 | 1.978 | 86.4 | 17.1 | −0.32 | 44.9 |
| MRCI | 69.428 88 | 1.963 | 87.9 | 26.8 | −0.34 | 58.2 |
| MRCI+Q[d] | 69.440 | 1.954 | 89.3 | 31 | | 56.8 |

[a] With respect to the ground-state products $N(^4S) + 2Li(^2S)$. [b] With respect to the ground $\tilde{X}^2\Pi_u$ state. [c] Single-reference Davidson correction for unlinked quadruples. [d] Multireference Davidson correction, ref 14. [e] Obtained from the $^2B_2$ state in the limit of $\theta = 180.0°$.

Now, there are two ways of taking the molecule apart: one by simultaneously stretching away the two Li atoms in a symmetric fashion maintaining the center of symmetry; the second by stretching away one Li atom with respect to the NLi fragment. The potential energy curves of these two modes of opening, symmetric (S) and asymmetric (A), are shown in Figure 2 with corresponding numerical results presented in Table 5. Both PECs were obtained by defining the $z$-axis to be the molecular axis. As we can see from Figure 2, the S-opening traces its lineage to one Li atom in the ground $^2S$ state and the other to the first excited $^2P$ state

$$NLi_2(\tilde{X}^2\Pi_u) \rightarrow Li(^2S) + Li(^2P) + N(^4S)$$

as it should. The atomization energy of the above process is 127.4 kcal/mol with respect to the $^2P$ state of Li (Table 5) or 84.9 kcal/mol with respect to the ground-state products (Table 3), at the MRCI level of theory. Therefore the mean dissociation N−Li energy is 84.9/2 = 42.5 kcal/mol, about 10 kcal/mol larger than the $D_e$ of NLi ($X^3\Sigma^-$), Table 2.

The A-opening mode correlates to the first excited $A^3\Pi$ state of NLi and the ground $^2S$ state of the Li atom

$$NLi_2(\tilde{X}^2\Pi_u) \rightarrow NLi(A^3\Pi) + Li(^2S)$$

(Figure 2) again as it should. The $D_e$ of this process with respect to the asymptotic products (internal bond strength) is 57.1 kcal/mol at the MRCI level (Table 5) or 57.1−5.3 = 51.8 kcal/mol (Table 2) with respect to the ground-state products, NLi ($X^3\Sigma^-$) + $Li(^2S)$. Both the S- and A-opening modes are in agreement with the binding mechanism of $NLi_2$ presented before.

**$PLi_2$, Ground $\tilde{X}^2B_1$ ($5a_1^26a_1^23b_2^22b_1^1$) State.** The single most important difference between the ground states of $NLi_2$ and $PLi_2$ molecules is that the former is linear while the latter is strongly bent, $\theta$ = 100° at the MRCI level (Table 4,

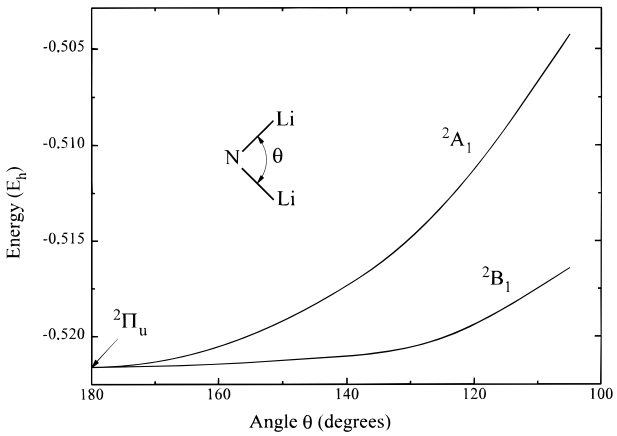


**Figure 1.** Splitting of the $NLi_2$ (linear) $\tilde{X}^2\Pi_u$ state as a function of the $\theta$ angle, MRCI level of theory.

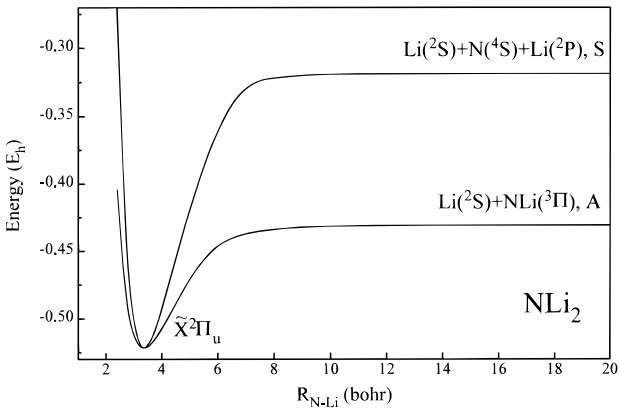


**Figure 2.** Symmetric (S) and asymmetric (A) PECs of $NLi_2$ in the linear $^2\Pi_u$ configuration, MRCI level of theory.

**TABLE 4: Absolute Energies $E$ (hartrees), Bond Lengths $r_e$ (angstroms), Angles $\theta$ (degrees ∠LiPLi), Binding Energies $D_e$ (kcal/mol), Mulliken Charges $q_P$, and Energy Differences $T_e$ (kcal/mol) of the Ground $\tilde{X}^2B_1$ State and Some Low-Lying Excited States of $PLi_2$**

| method | $-E$ | $r_e$ | $\theta$ | $D_e$[a] | $q$ | $T_e$[b] | method | $-E$ | $r_e$ | $\theta$ | $D_e$[a] | $q$ | $T_e$[b] |
|---|---|---|---|---|---|---|---|---|---|---|---|---|---|
| | | $\tilde{X}^2B_1$ | | | | | | | $^2\Sigma_g^-$ | | | | |
| SCF | 355.639 49 | 2.264 | 116.6 | 35.0 | −0.51 | | SCF | 355.618 90 | 2.439 | 180.0 | 22.1 | −0.25 | 12.9 |
| CISD | 355.803 54 | 2.264 | 114.2 | 72.9 | −0.49 | | CISD | 355.756 14 | 2.439 | 180.0 | 43.2 | −0.24 | 29.8 |
| CISD+Q[c] | 355.820 | 2.272 | 111.2 | 79 | | | CISD+Q[c] | 355.768 | 2.445 | 180.0 | 46 | | 32.5 |
| CASSCF | 355.685 35 | 2.297 | 102.0 | 55.1 | −0.52 | | CASSCF | 355.642 97 | 2.473 | 180.0 | 28.5 | −0.23 | 26.6 |
| MRCI | 355.817 36 | 2.291 | 100.0 | 80.4 | −0.47 | | MRCI | 355.761 93 | 2.450 | 180.0 | 45.8 | −0.24 | 34.8 |
| MRCI+Q[d] | 355.829 | 2.297 | 98.3 | 84 | | | MRCI+Q[d] | 355.772 | 2.454 | 180.0 | 48 | | 36.0 |
| MRCI+Q[e] | 355.801 14 | 2.267 | 112.0 | | | | | | | | | | |
| | | $^2\Pi_u$[f] | | | | | | | $^4\Sigma_u^-$ | | | | |
| SCF | 355.638 59 | 2.231 | 180.0 | 34.4 | −0.51 | 0.6 | SCF | 355.609 07 | 2.431 | 180.0 | 15.9 | −0.28 | 19.1 |
| CISD | 355.802 75 | 2.229 | 180.0 | 72.4 | −0.50 | 0.5 | CISD | 355.748 82 | 2.424 | 180.0 | 38.6 | −0.26 | 34.3 |
| CISD+Q[c] | 355.819 | 2.232 | 180.0 | 78.2 | | 0.8 | CISD+Q[c] | 355.761 | 2.429 | 180.0 | 42 | | 36.9 |
| CASSCF | 355.681 22 | 2.225 | 180.0 | 52.5 | −0.53 | 2.6 | CASSCF | 355.640 04 | 2.418 | 180.0 | 26.7 | −0.26 | 28.4 |
| MRCI | 355.813 49 | 2.230 | 180.0 | 78.1 | −0.50 | 2.4 | MRCI | 355.755 59 | 2.425 | 180.0 | 41.8 | −0.25 | 38.8 |
| MRCI+Q[d] | 355.825 | 2.234 | 180.0 | 82 | | 2.6 | MRCI+Q[d] | 355.765 | 2.432 | 180.0 | 44 | | 40.4 |
| | | $^2B_2$ | | | | | | | $^2\Sigma_u^-$ | | | | |
| SCF | 355.614 02 | 2.256 | 83.6 | 19.0 | −0.55 | 16.0 | SCF | 355.607 56 | 2.425 | 180.0 | 15.0 | −0.29 | 20.0 |
| CISD | 355.783 03 | 2.261 | 82.4 | 60.1 | −0.50 | 12.9 | CISD | 355.747 27 | 2.421 | 180.0 | 37.6 | −0.27 | 35.3 |
| CISD+Q[c] | 355.801 | 2.272 | 81.3 | 67 | | 11.7 | CISD+Q[c] | 355.759 | 2.425 | 180.0 | 41 | | 38.0 |
| CASSCF | 355.666 95 | 2.296 | 76.7 | 43.6 | −0.45 | 11.6 | CASSCF | 355.638 77 | 2.418 | 180.0 | 25.9 | −0.28 | 29.2 |
| MRCI | 355.798 38 | 2.286 | 78.2 | 68.7 | −0.47 | 11.9 | MRCI | 355.754 03 | 2.422 | 180.0 | 40.8 | −0.26 | 39.7 |
| MRCI+Q[d] | 355.810 | 2.288 | 78.3 | 72 | | 12.1 | MRCI+Q[d] | 355.763 | 2.426 | 180.0 | 43 | | 41.5 |
| | | $^2\Sigma_u^+$[g] | | | | | | | $^2A_1$ | | | | |
| SCF | 355.592 13 | 2.177 | 180.0 | | −0.56 | 29.7 | SCF | 355.581 58 | 2.497 | 66.9 | −1.3 | −0.29 | 36.3 |
| CISD | 355.760 52 | 2.170 | 180.0 | | −0.53 | 27.0 | CISD | 355.734 54 | 2.489 | 67.4 | 29.6 | −0.28 | 43.3 |
| CISD+Q[c] | 355.778 | 2.173 | 180.0 | | | 26.5 | CISD+Q[c] | 355.751 | 2.490 | 67.4 | 36 | | 43.1 |
| CASSCF | 355.644 02 | 2.151 | 180.0 | | −0.54 | 25.9 | CASSCF | 355.620 61 | 2.508 | 66.1 | 14.5 | −0.26 | 40.6 |
| MRCI | 355.773 24 | 2.166 | 180.0 | | −0.52 | 27.7 | MRCI | 355.743 59 | 2.486 | 67.3 | 34.3 | −0.24 | 46.3 |
| MRCI+Q[d] | 355.784 | 2.172 | 180.0 | | | 28.4 | MRCI+Q[d] | 355.758 | 2.489 | 67.4 | 40 | | 44.9 |
| | | $^4\Sigma_g^-$ | | | | | | | | | | | |
| SCF | 355.619 37 | 2.429 | 180.0 | 22.4 | −0.24 | 12.6 | | | | | | | |
| CISD | 355.761 32 | 2.427 | 180.0 | 46.4 | −0.21 | 26.5 | | | | | | | |
| CISD+Q[c] | 355.774 | 2.433 | 180.0 | 50 | | 28.7 | | | | | | | |
| CASSCF | 355.649 59 | 2.419 | 180.0 | 32.7 | −0.23 | 22.4 | | | | | | | |
| MRCI | 355.768 17 | 2.427 | 180.0 | 49.7 | −0.21 | 30.9 | | | | | | | |
| MRCI+Q[d] | 355.778 | 2.435 | 180.0 | 52.5 | | 32.0 | | | | | | | |

[a] With respect to the ground-state products $P(^4S) + 2Li(^2S)$. [b] With respect to the ground $\tilde{X}^2B_1$ state. [c] Single-reference Davidson correction for unlinked quadruples. [d] Multireference Davidson correction, ref 14. [e] Reference 2. ANO-basis set, $(17s12p5d4f/(14s9p4d3f)_2) \rightarrow [5s4p2d/(4s3p2d)_2]$. MRCI+Full CI Davidson correction. [f] Obtained from the $\tilde{X}^2B_1$ state in the limit of $\theta = 180.0°$, $\tilde{X}^2B_1 \rightarrow {}^2\Pi_u(^2B_1,{}^2A_1)$. [g] Obtained from the $^2B_2$ state in the limit of $\theta = 180.0°$.

**TABLE 5: Dissociation Energies $D_e$ (kcal/mol) with Respect to Asymptotic Fragments of $NLi_2$ ($\tilde{X}^2\Pi_u$) and $PLi_2$ ($\tilde{X}^2B_1$, $^2\Pi_u$)**

| | $NLi_2$ | | $PLi_2$ | | |
|---|---|---|---|---|---|
| | $\tilde{X}^2\Pi_u$ | | $^2\Pi_u$ | | $\tilde{X}^2B_1$ |
| method | $D_e$-A[a] | $D_e$-S[b] | $D_e$-A[c] | $D_e$-S[d] | $D_e$-S[e] |
| CASSCF | 50.5 | 104.5 | 42.6 | 82.6 | 55.1 |
| MRCI | 57.1 | 127.4 | 55.4 | 112.3 | 80.4 |
| MRCI+Q[f] | 58 | 131 | 57.4 | 117 | 84 |

[a] Asymmetric opening, $NLi_2(\tilde{X}^2\Pi_u) \rightarrow NLi(A^3\Pi) + Li(^2S)$. [b] Symmetric opening, $NLi_2(\tilde{X}^2\Pi_u) \rightarrow Li(^2S) + Li(^2P) + N(^4S)$. [c] Asymmetric opening, $PLi_2(^2\Pi_u) \rightarrow PLi(A^3\Pi) + Li(^2S)$. [d] Symmetric opening, $PLi_2(^2\Pi_u) \rightarrow 2Li(^2S) + P(^2D)$. [e] Angular symmetric opening, $PLi_2(\tilde{X}^2B_1) \rightarrow 2Li(^2S) + P(^4S)$. [f] Multireference Davidson correction, ref 14.

Figure 3). In the linear $^2\Pi_u$ configuration exactly the same binding mechanism operates as in $NLi_2$, with the one in situ Li atom in the $^2P$ state and the other in the ground $^2S$ state as described before. As we bend the molecule in a $^2B_1$ fashion, the total energy falls very slowly till it reaches a minimum at $\theta = 100°$, with an energy gaining (inversion barrier) of 2.4 kcal/mol at equilibrium (Table 4, Figure 3). Despite the very small energy difference between the bent and the linear geometries (the molecule in essence is quasilinear), $PLi_2$ is predicted to be formally bent at all levels of theory, even at the SCF (Table 4). Figure 3 presents the $^2\Pi_u \rightarrow {}^2B_1$ PEC along with the $^2\Pi_u \rightarrow {}^2A_1$ PEC. Certainly in the $\tilde{X}^2B_1$ state the binding appears to be quite different from that in the linear $^2\Pi_u$ case, the prevailing valence bond−Lewis icon in this state being i.e., two $\sigma$-bonds

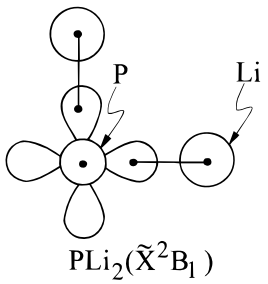

$PLi_2(\tilde{X}^2B_l)$

originating from the ground state of P and Li atoms, assisted with small promotions to the Li $p_y$- and $p_z$-orbitals. From Table 4 we also observe a significant bond length difference between the bent and the linear configurations, the latter being shorter by 0.06 Å, reflecting the different bonding character between the two cases, bent vs linear.

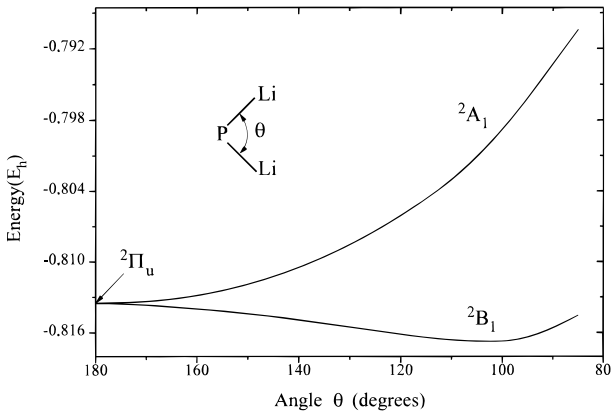


**Figure 3.** Splitting of the $PLi_2$ (linear) $^2\Pi_u$ state as a function of the $\theta$ angle, MRCI level of theory.

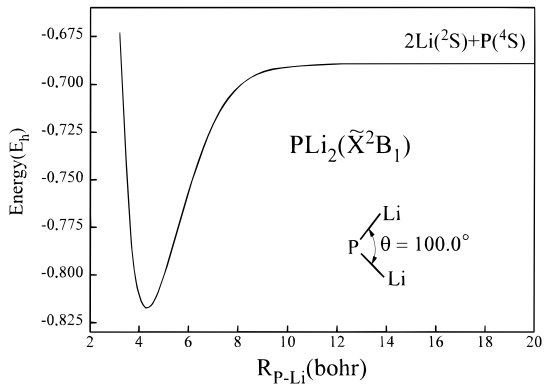


**Figure 4.** Potential energy curve of $PLi_2$ in the $\tilde{X}^2B_1$ ($\theta = 100°$), MRCI level of theory.

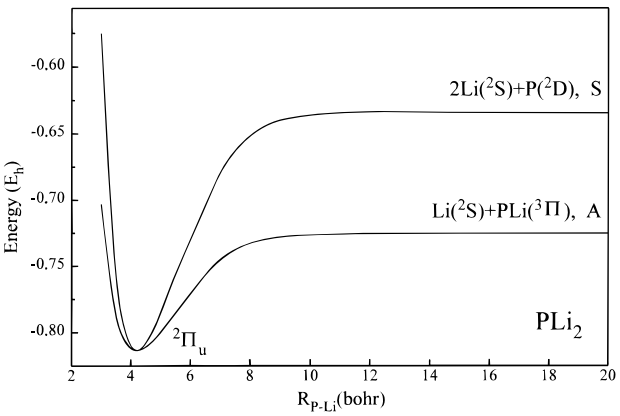


**Figure 5.** Symmetric (S) and asymmetric (A) PECs of $PLi_2$ ($^2\Pi_u$ at $\theta = 180°$), MRCI level of theory.

Now, as we take the molecule apart in a symmetric fashion, maintaing the $C_{2v}$ symmetry and a LiPLi angle of 100°, we end up with the ground-state fragments, $2Li(^2S) + P(^4S)$, obtaining a mean P−Li binding energy of 80.4/2 = 40.2 kcal/mol at the MRCI level (Table 5). The corresponding PEC, $PLi_2$ ($\tilde{X}^2B_1$) → $2Li(^2S) + P(^4S)$, $\theta = 100°$, is shown in Figure 4.

As in the $NLi_2$ case the $PLi_2$ in its linear $^2\Pi_u$ configuration ($^2B_1 \rightarrow {}^2\Pi_u$), can be thought as the result of either the PLi($A^3\Pi$) + Li($^2S$) or the PLi($X^3\Sigma^-$) + Li($^2P$) process (vide supra). By pulling apart a Li atom, i.e., breaking a PLi−Li bond (A-mode), the PEC of Figure 5 is obtained, with products PLi($A^3\Pi$) + Li($^2S$). This is of course expected because the $A^3\Pi \leftarrow X^3\Sigma^-$ energy difference of PLi is smaller than the $^2P \leftarrow {}^2S$ energy difference of the Li atom, 13.7 kcal/mol (Table 2) vs 42.5 kcal/mol, respectively. The resulting PLi−Li $D_e$ with

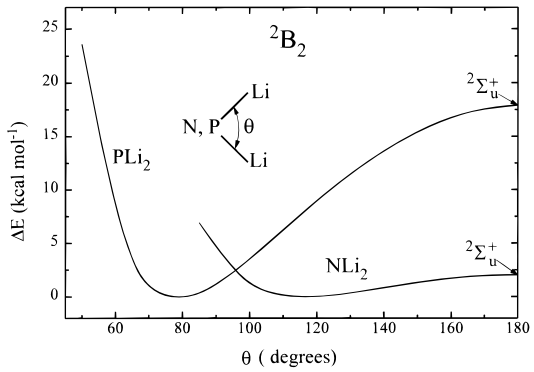


**Figure 6.** Potential energy curves (relative energies) of $NLi_2$ and $PLi_2$ in the $^2B_2$ state(s) with respect to the $\theta$ angle, MRCI level of theory.

respect to the ground-state fragments PLi($A^3\Sigma^-$) + Li($^2S$) is 55.4−13.7 = 41.7 kcal/mol (Table 5, MRCI level). Correcting this value for the opening ($\tilde{X}^2B_1 \rightarrow {}^2\Pi_u$) energy loss of 2.4 kcal/mol (Table 4), the PLi−Li binding energy $D_e$ is 44.1 kcal/mol. By pulling the molecule apart in an S-fashion (linearly), $PLi_2 \rightarrow 2Li + P$, the PEC of Figure 5 is obtained with end fragments $2Li(^2S) + P(^2D)$. Here the situation differs from the corresponding $NLi_2$ case (Figure 2), where the end products are Li($^2S$) + Li($^2P$) + N($^4S$), due to an avoided crossing between the Li($^2S$) + Li($^2P$) + P($^4S$) and $2Li(^2S) + P(^2D)$ PECs: the $^2D$ state of the P atom is 8.2 kcal/mol (10.0 kcal/mol experimentally[15]), lower than the $^2P$ state of the Li atom.

Finally, $PLi_2$ is as ionic as $NLi_2$ ($^2\Pi_u$) in both its bent ($\tilde{X}^2B_1$) or linear ($^2\Pi_u$) geometry, with a total of ∼0.5 $e^-$ transferred to the P atom (Table 4).

**$NLi_2$, $PLi_2$, $^2B_2$.** The $^2B_2$ states of $NLi_2$ ($3a_1^2 4a_1^2 1b_1^2 2b_2^1$) and $PLi_2$ ($5a_1^2 6a_1^2 2b_1^2 3b_2^1$) species are 9.7 and 11.9 kcal/mol, respectively, above their ground states. Both are practically equally bound with respect to their ground-state atoms, with mean N−Li and P−Li binding energies of 37.7 and 34.4 kcal/mol (MRCI, Tables 3 and 4). However the LiPLi angle is 30° smaller than the LiNLi angle. In addition, $NLi_2$ is a floppy system having an inversion barrier of just 2.2 kcal/mol as compared to 17.2 kcal/mol of $PLi_2$ (MRCI). The PECs of the two systems as functions of $\theta$, keeping the bond lengths constant at their equilibrium values, are shown in Figure 6 with both systems ending up in a $^2\Sigma_u^+$ symmetry. The valence bond−Lewis pictures of the binding scheme in the *linear* $^2\Sigma_u^+$ configuration is quite interesting with the in situ N or P atoms

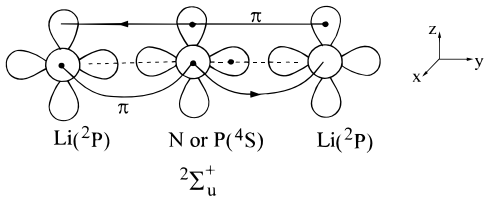


in the ground $^4S$ state and the in situ Li atoms in the excited $^2P$ state. The CAS atomic populations are clearly in support of the above picture as the main bonding scheme in the linear geometry

$$NLi_2: \quad 2s^{1.69}2p_x^{1.41}2p_y^{0.82}2p_z^{1.41}/2s^{0.08}2p_x^{0.22}2p_y^{0.06}2p_z^{0.30}$$

$$PLi_2: \quad 3s^{1.63}3p_x^{1.61}3p_y^{0.67}3p_z^{1.60}/2s^{0.15}2p_x^{0.14}2p_y^{0.07}2p_z^{0.24}$$

where the first entry refers to the N or P populations and the second to the Li populations. In other words, in the (linear)

$^2\Sigma_u^+$ configuration the molecules are held together by two 3-center-2-electron $\pi$-bonds perpendicular to each other and a 3-center-1-electron $\sigma$-bond. This strong delocalization of the $\pi$-system is also the cause of the significant shortening of the bond lengths in the $^2\Sigma_u^+$ configurations, as compared to the $^2B_2$ states, by 0.05 and 0.11 Å for the $NLi_2$ and $PLi_2$, respectively (MRCI, Tables 3 and 4).

**$NLi_2$, $PLi_2$, $^4\Sigma_g^-(^4B_1)$ $3\sigma_g^2 4\sigma_g^1 1\pi_u^2 2\sigma_u^2$ and $5\sigma_g^2 6\sigma_g^1 2\pi_u^2 3\sigma_u^2$ ($3a_1^2 4a_1^1 2b_2^2 5a_1^1 1b_1^1$, $5a_1^2 6a_1^1 3b_2^2 7a_1^1 2b_1^1$).** We can imagine the formation of the $^4\Sigma_g^-$ state of either the $NLi_2$ or $PLi_2$ systems as taking place by the approach of a ground $^2S$ Li atom from infinity to the ground $X^3\Sigma^-$ state of NLi or PLi while coupling the three electrons into a quartet, $NLi(X^3\Sigma^-) + Li(^2S) \rightarrow NLi_2(^4\Sigma_g^-)$. The prevailing valence bond−Lewis icon gives a clear representation of the "bonding" interaction:

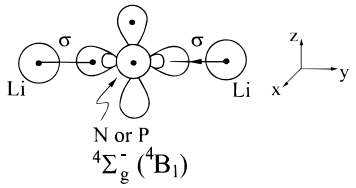


The symmetry of the system imposes the coexistence of the mirror image of the above icon in the equilibrium, so the two Li atoms are strictly equivalent with a 3-center-3-electron bond along the $\sigma$-frame ($y$-axis). The equilibrium CAS atomic populations are revealing:

$$NLi_2: \quad 2s^{1.84}2p_x^{0.96}2p_y^{1.59}2p_z^{0.96}/2s^{0.59}2p_x^{0.01}2p_y^{0.09}2p_z^{0.08}$$

$$PLi_2: \quad 3s^{1.79}3p_x^{0.96}3p_y^{1.51}3p_z^{0.96}/2s^{0.64}2p_x^{0.01}2p_y^{0.06}2p_z^{0.09}$$

Grossly 0.5 $e^-$ are transferred to the N or P atoms through the $\sigma$-frame with a concomitant ~0.2 $e^-$ transfer from N or P atoms to the $p_y$, $p_z$ atomic-like orbitals of the Li atoms.

This state is bound with respect to the ground-state atoms by 61.3 ($NLi_2$) and 49.7 ($PLi_2$) kcal/mol (MRCI, Tables 3 and 4) or mean binding energies, N−Li and P−Li of ~31 and 25 kcal/mol, respectively. This nature of interaction dictates large bond lengths, and indeed we have for both molecules a bond lengthening of 0.14 Å as compared to the ground states (MRCI). It is remarkable that in the $NLi_2$ system and at the SCF level the $^4\Sigma_g^-$ state is *lower* in energy by 10.5 kcal/mol than the ground $\tilde{X}^2\Pi_u$ state. It is obvious that the SCF wave function gives a qualitatively correct description of this state, and of course we can even separate correctly one Li atom at the Hartree−Fock level. The PECs of $NLi_2(^4\Sigma_g^-) \rightarrow NLi(X^3\Sigma^-) + Li(^2S)$ and $PLi_2(^4\Sigma_g^-) \rightarrow PLi(X^3\Sigma^-) + Li(^2S)$ at the MRCI level are shown in Figures 7 and 8, with $D_e$ values of 28.0 and 13.3 kcal/mol, respectively. These numbers should be contrasted with the mean $D_e$ values previously reported of 31 and 25 kcal/mol.

**$NLi_2$, $PLi_2$, $^4\Sigma_u^-$, ($^4A_2$; $3a_1^2 4a_1^1 2b_2^2 3b_2^1 1b_1^1$, $5a_1^2 6a_1^1 3b_2^2$-$4b_2^1 2b_1^1$).** By alloting the $5a_1(4\sigma_g)$ electron of the $NLi_2$ $^4\Sigma_g^-$ state to a $3b_2(3\sigma_u)$ symmetry orbital, the $^4\Sigma_u^-$ state is obtained, i.e., $3\sigma_g^2 1\pi_u^2 2\sigma_u^2 3\sigma_u^1$. Mutatis mutandis the same is true for the $PLi_2$ system. As a result the $^4\Sigma_u^-$ state for both molecules is similar in every respect to the $^4\Sigma_g^-$ state: bond lengths, bonding character, ionicity, and CAS populations are practically the same between the two states. The only difference between the $^4\Sigma_u^-$ and the $^4\Sigma_g^-$ states is that the former has a ~8 kcal/mol smaller binding energy (atomization energy) with respect to the ground-state atoms (MRCI, Tables 3, 4), for both molecular systems.

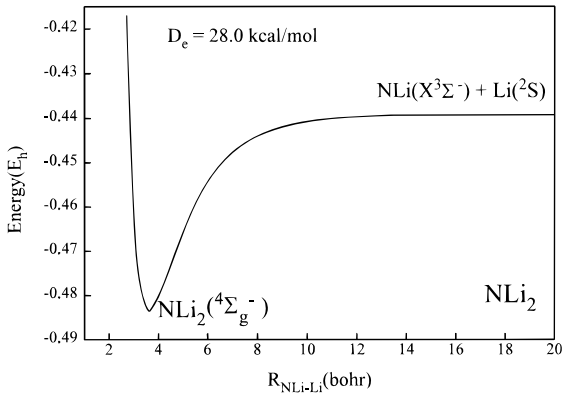


**Figure 7.** MRCI PEC of the NLi−Li bond-breaking process, $^4\Sigma_g^-$ state.

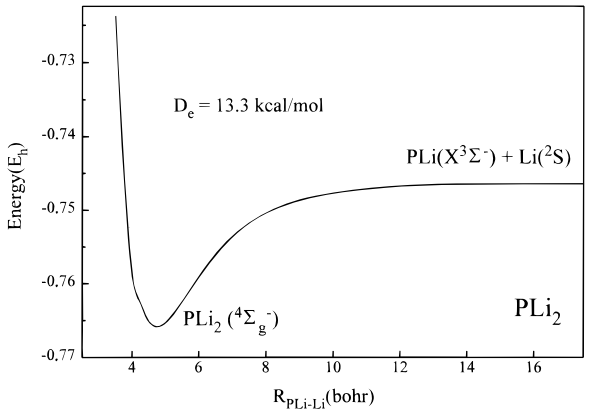


**Figure 8.** MRCI PEC of the PLi−Li bond-breaking process, $^4\Sigma_g^-$ state.

**$NLi_2$, $PLi_2$, $^2\Sigma_g^-(^2A_2)$.** In both molecules the bonding originates from the first excited $^2D(M=0)$ state of N or P. The calculated MRCI level energy differences $\Delta E(^2D \leftarrow ^4S)$ for the N and P atoms are 2.457 and 1.484 eV, respectively, with corresponding experimental values of 2.384 and 1.410 eV.[15] The valence bond−Lewis cartoon representing the main features of binding is

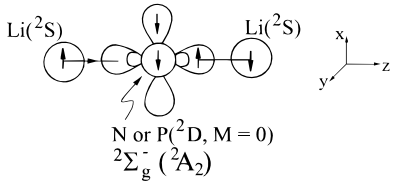


The situation differs from the $^4\Sigma_g^-$ state of $NLi_2$ or $PLi_2$ by one spin-flip on the N or P atoms, resulting in a more complicated description of the leading configuration. At the CASSCF level the leading configurations of $NLi_2$ and $PLi_2$ have the following electron allocations (notice that the molecular axis is the $z$-axis):

$$NLi_2: \quad {}^2\Sigma_g^-({}^2A_2) = 1/6^{1/2}[(4a_1)^2(5a_1)^2(1b_1)^1(1b_2)^1(6a_1)^1] \\ (2\alpha\alpha\beta - \alpha\beta\alpha - \beta\alpha\alpha)$$

$$PLi_2: \quad {}^2\Sigma_g^-({}^2A_2) = 1/6^{1/2}[(6a_1)^2(7a_1)^2(2b_1)^1(2b_2)^1(8a_1)^1] \\ (2\alpha\alpha\beta - \alpha\beta\alpha - \beta\alpha\alpha)$$

The equilibrium CAS atomic populations are

$NLi_2$: $2s^{1.84}2p_x^{0.96}2p_y^{0.96}2p_z^{1.58}/2s^{0.55}2p_x^{0.01}2p_y^{0.01}2p_z^{0.21}$

$PLi_2$: $3s^{1.79}3p_x^{0.97}3p_y^{0.97}3p_z^{1.44}/2s^{0.60}2p_x^{0.0}2p_y^{0.0}2p_z^{0.25}$

corroborating the previous given icon. Clearly, the $\pi$ $p_{x,y}$ electrons of N or P atoms remain intact, while the 3-electron-3-center $\sigma$-bond is assisted by transfer of $\sim$0.4 $e^-$ via the $\sigma$-frame from the Li atoms to the N or P atoms. From Tables 3 and 4 the similarity between the $^4\Sigma_g^-$ and $^2\Sigma_g^-$ states is clear: for both molecules the $D_e$ values with respect to the ground-state products of the $^2\Sigma_g^-$ state are smaller by less than 4 kcal/mol than the $D_e$ values of the $^4\Sigma_g^-$ state, while the bond distances lengthen by only approximately 0.01 and 0.02 Å in $NLi_2$ and $PLi_2$, respectively, as compared to the $^4\Sigma_g^-$ state.

**$NLi_2$, $PLi_2$, $^2\Sigma_u^-(^2A_2)$.** The situation here is very similar to the previously discussed $^2\Sigma_g^-$ state. The same valence bond−Lewis icon describes the binding scheme, but this time the *y*-axis is the molecular axis with *z* being the 2-fold axis. The leading configurations of the CASSCF wave functions are

$NLi_2$: $^2\Sigma_u^-(^2A_2) = 1/6^{1/2}[(3a_1)^2(4a_1)^1(2b_2)^2(1b_1)^1(3b_2)^1]$ $(2\alpha\alpha\beta-\alpha\beta\alpha-\beta\alpha\alpha)$

$PLi_2$: $^2\Sigma_u^-(^2A_2) = 1/6^{1/2}[(5a_1)^2(6a_1)^1(3b_2)^2(2b_1)^1(4\,b_2)^1]$ $(2\alpha\alpha\beta-\alpha\beta\alpha-\beta\alpha\alpha)$

The equilibrium CAS atomic populations are practically the same as those of the $^2\Sigma_g^-$ state for both molecules (remember that *y* is the molecular axis)

$NLi_2$: $2s^{1.84}2p_x^{0.96}2p_y^{1.60}2p_z^{0.96}/2s^{0.36}2p_x^{0.01}2p_y^{0.28}2p_z^{0.05}$

$PLi_2$: $3s^{1.81}3p_x^{0.97}3p_y^{1.49}3p_z^{0.97}/2s^{0.44}2p_x^{0.01}2p_y^{0.31}2p_z^{0.05}$

From Tables 3 and 4 we observe that the similarities between the $^4\Sigma_u^-$ and the $^2\Sigma_u^-$ states of $NLi_2$ and $PLi_2$ systems are strikingly independent of the level of calculation. At the MRCI level for both molecules the $D_e$ values with respect to ground-state products differ by just 1 kcal/mol while the bond distances by less than 0.005 Å between the $^4\Sigma_u^-$ and $^2\Sigma_u^-$ states.

**$NLi_2$, $PLi_2$, $^2A_1$.** ($3a_1^24a_1^25a_1^12b_2^2$, $5a_1^26a_1^27a_1^13b_2^2$) These are severely bent states, particularly in the $PLi_2$ system, with LiNLi and LiPLi angles of $\sim$90° and $\sim$67° at all levels of calculation and with $D_e$ values, with respect to the ground-state products of 26.8 and 34.3 kcal/mol, respectively, at the MRCI level of theory (Tables 3 and 4). This is the only state in which the $NLi_2$ species is *unbound* with respect to NLi ($X^3\Sigma^-$) + Li-($^2$S) fragments, Table 3. The bonding arises from the first excited $^2$D state of N or P atoms and the ground $^2$S state of the Li atoms, but the binding scheme is not that clear. The CAS atomic populations are as follows

$NLi_2$: $2s^{1.84}2p_x^{0.0}2p_y^{1.71}2p_z^{1.77}/2s^{0.47}2p_x^{0.0}2p_y^{0.08}2p_z^{0.24}$

$PLi_2$: $3s^{1.87}3p_x^{0.0}3p_y^{1.69}3p_z^{1.63}/2s^{0.47}2p_x^{0.0}2p_y^{0.06}2p_z^{0.28}$

It is interesting that the Li−Li distance within the $NLi_2$ and $PLi_2$ systems is 2.725 and 2.756 Å at the MRCI level, as compared to 2.703 Å of the dilithium molecule $Li_2(^1\Sigma_g^+)$ at the CISD level.

A consistent cartoon with these findings can be drawn as follows

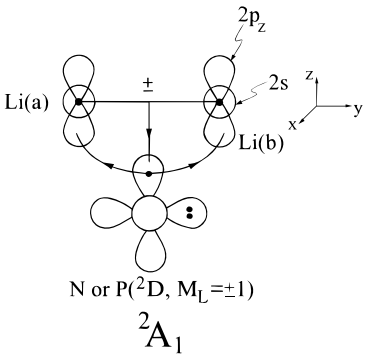


$^2A_1$

The plus sign of the above cartoon corresponds to a molecular orbital of $a_1$ symmetry and the minus sign to an "antibonding" molecular orbital (MO) of $b_2$ symmetry, while the $p_y$ electron pair on N or P atoms is of $b_2$ symmetry as well. Therefore we can imagine that the bonding is due to a delocalization of the single $p_z$ (N or P) electron into the $2p_z(a) + 2p_z(b)$ MO, with a concomitant donation of electrons from the $\sigma$-bond ($\sim 2s_a + 2s_b$) of $Li_2$. At the same time the N or P $b_2$ pair can interact with the antibonding system of the $Li_2$ moiety. This picture is in accord with the CAS atomic populations reported previously.

## 4. Synopsis and Final Remarks

We have examined by ab initio CISD and MRCI techniques, the ground states $\tilde{X}^2\Pi_u$ and $\tilde{X}^2B_1$ and certain low-lying excited states of the $NLi_2$ and $PLi_2$ isovalent species. All states studied, and for both molecules, are bound with respect to the ground-state atoms, N or P($^4$S) + 2Li($^2$S). With the exception of the $NLi_2$ $^2A_1$ state, all states for both molecules are also bound with respect to the ground-state fragments NLi or PLi($X^3\Sigma^-$) + Li-($^2$S). In addition, all states show ionic character with a total transfer of 0.2−0.5 electrons from the two Li to N or P atoms, depending on the state.

The ground state of $NLi_2$ is linear with a $^2\Pi_u$ symmetry and very floppy, while the $PLi_2$ system, albeit also very floppy, is strongly bent ($\theta = 100°$) with a ground state of $^2B_1$ symmetry and an energy inversion barrier of 2.4 kcal/mol.

At the MRCI level of theory the binding values of $NLi_2$ ($\tilde{X}^2\Pi_u$) and $PLi_2(\tilde{X}^2B_1)$ are NLi−Li = 51.8 kcal/mol, N−Li (mean) = 42.5 kcal/mol and PLi−Li = 44.1 kcal/mol, P−Li (mean) = 40.2 kcal/mol. The above values should be compared with the $D_e$ values of the ground-state diatomics NLi($X^3\Sigma^-$) and PLi($X^3\Sigma^-$) of 33.3 and 36.3 kcal/mol, respectively.

We observe that while the mean binding energies N−Li and P−Li are similar, there is an apparent difference between the NLi−Li and PLi−Li dissociation energies. This is due to the difference in the energy splittings ($T_e$) $A^3\Pi \leftarrow X^3\Sigma^-$ of NLi and PLi, 5.3 and 13.7 kcal/mol, respectively (MRCI). Comparing the *internal bond strengths*, i.e., dissociation energies for the reactions $NLi_2(\tilde{X}^2\Pi_u) \rightarrow NLi(A^3\Pi) + Li(^2S)$ and $PLi_2(^2\Pi_u) \rightarrow PLi(A^3\Pi) + Li(^2S)$, the $D_e$ values are 57.1 and 55.4 kcal/mol for the NLi−Li and PLi−Li bonds, respectively. Correcting the 55.4 kcal/mol value by 2.4 kcal/mol due to the energy loss $\tilde{X}^2B_1 \rightarrow {}^2\Pi_u$, the PLi−Li internal bond strength becomes 57.8 kcal/mol in practical agreement with the NLi−Li value.

Now, it is of interest to compare the bond length of the ground $^3\Sigma^-$ state of NLi with the corresponding $\tilde{X}^2\Pi_u$ of $NLi_2$. At the MRCI level a large bond shortening of 0.103 Å of $NLi_2$ is observed as compared to the bond length of the NLi species, reflecting the difference in the bonding character between the two systems. Using conventional chemical drawings, the two systems can be represented as follows making clear the reason

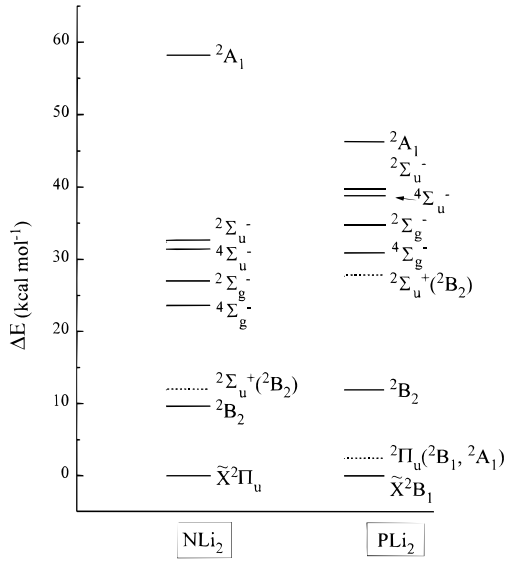


**Figure 9.** Relative energy diagram for all states computed of the $NLi_2$ and $PLi_2$ species, MRCI level of theory. Dashed levels represent corresponding linear geometries, $^2B_2 \rightarrow {}^2\Sigma_u^+$ ($NLi_2$, $PLi_2$) and $\tilde{X}^2B_1 \rightarrow {}^2\Pi_u$ ($PLi_2$).


of bond shortening in the triatomic molecule. The same is true for the $PLi_2$, PLi systems, but the contrast should be made between the ground $X^3\Sigma^-$ state of PLi and the $^2\Pi_u$ linear configuration of $PLi_2$, not its ground $\tilde{X}^2B_1$ state where the bonding character changes drastically. The bond shortening between PLi($X^3\Sigma^-$) and $PLi_2(^2\Pi_u)$ is 0.107 Å, with the latter being shorter exactly as in the $NLi_2-$NLi case and with the same rationalization.

Finally, Figure 9 shows an energy diagram summarizing relative energy levels for all states and geometries studied for both systems.

**Acknowledgment.** D.T. expresses her sincere gratitude to the State Scholarship Foundation (IKY) for economic assistance.

## References and Notes

(1) Kudo, H.; Zmbov, K. F. *Chem. Phys. Lett.* **1991**, *187*, 77.

(2) Kudo, H. Personal communication. We thank Professor Kudo for providing us with some of his unpublished results on the $PLi_2$ and PLi systems.

(3) See, for instance: Nazri, G. *Solid State Ionics* **1989**, *34*, 97 and references therein.

(4) (a) Tzeli, D.; Papakondylis, A.; Mavridis, A. *J. Mol. Struct.* (*THEOCHEM*) **1997**, *417* (3), 281−291. (b) Matsika, S.; Papakondylis, A.; Mavridis, A. *Chem. Phys. Lett.* **1996**, *250*, 409. (c) Kalemos, A.; Papakondylis, A.; Mavridis, A. *Chem. Phys. Lett.* **1996**, *259*, 185. (d) Kalemos, A.; Papakondylis, A.; Mavridis, A. *J. Mol. Struct.* (*THEOCHEM*) **1995**, *357*, 97. (e) Mavridis, A.; Harrison, J. F. *J. Phys. Chem.* **1982**, *86*, 1979. (f) Mavridis, A.; Harrison, J. F. *J. Am. Chem. Soc.* **1982**, *104*, 3827.

(5) Dunning, T. H., Jr. *J. Chem. Phys.* **1989**, *90*, 1007.

(6) Woon, D. E.; Dunning, T. H., Jr. *J. Chem. Phys.* **1993**, *98*, 1358.

(7) See, for instance: Peterson, K. A.; Dunning, T. H., Jr. *J. Chem. Phys.* **1997**, *106*, 4119. Xantheas, S. S.; Dunning, T. H., Jr.; Mavridis, A. *J. Chem. Phys.* **1997**, *106*, 3280.

(8) Shepard, R.; Shavitt, I.; Pitzer, R. M.; Comeau, D. C.; Pepper, M.; Lischka, H.; Szalay, P. G.; Ahlrichs, R.; Brown, F. B.; Zhao, J.-G. *Int. J. Quantum Chem.* **1988**, *S22*, 149.

(9) Davidson, E. R. *MELD*; Department of Chemistry, Indiana University: Bloomington, IN, 1991.

(10) MOLPRO is a package of ab initio programs written by Werner, H.-J. and Knowles, P. J. with contributions from Almlof, J.; Amos, R. D.; Berning, A.; Deegan, M. J. O.; Eckert, F.; Elbert, S. T.; Hampel, C.; Lindh, R.; Meyer, W.; Nicklass, A.; Peterson, K.; Pitzer, R.; Stone, A. J.; Taylor, P. R.; Mura, M. E.; Pulay, P.; Schuetz, M.; Stoll, H.; Thorsteinsson, T.; and Cooper, D. L.

(11) Werner, H.-J.; Knowles, P. J. *J. Chem. Phys.* **1994**, *89*, 3018. Knowles, P. J.; Werner, H.-J. *Chem. Phys. Lett.* **1988**, *145*, 514. Werner, H.-J.; Reinsch, E. A. *J. Chem. Phys.* **1982**, *76*, 3144. Werner, H.-J. *Adv. Chem. Phys.* **1987**, *69*, 1.

(12) Dykstra, C. E.; Pearson, P. K.; Schaefer, H. F., III. *J. Am. Chem. Soc.* **1975**, *97*, 2321.

(13) (a) Boldyrev, A. I.; Simons, J.; Schleyer, P. v. R. *J. Chem. Phys.* **1993**, *99*, 8793. (b) Boldyrev, A. I.; Simons, J. *J. Phys. Chem.* **1993**, *97*, 6149.

(14) Blomberg, M. R. A.; Sieghbahn, P. E. M. *J. Chem. Phys.* **1983**, *78*, 5682.

(15) Moore, C. E. Atomic Energy Levels in: Natl. Stand. Ref. Data Ser., US Natl. Bur. Stand., Cir 35, 1973.